Evidence for Eight-Node Mixed-Symmetry Superconductivity in a Correlated Organic Metal

Daniel Guterding,[1] Sandra Diehl,[2,3] Michaela Altmeyer,[1] Torsten Methfessel,[3] Ulrich Tutsch,[4] Harald Schubert,[4] Michael Lang,[4] Jens Müller,[4] Michael Huth,[4] Harald O. Jeschke,[1] Roser Valentí,[1] Martin Jourdan,[3] and Hans-Joachim Elmers[3,*]

[1]*Institut für Theoretische Physik, Goethe-Universität Frankfurt, Max-von-Laue-Strasse 1, 60438 Frankfurt am Main, Germany*

[2]*Graduate School Materials Science in Mainz, Staudingerweg 9, 55128 Mainz, Germany*

[3]*Institut für Physik, Johannes Gutenberg-Universität Mainz, Staudingerweg 7, 55128 Mainz, Germany*

[4]*Physikalisches Institut, Goethe-Universität Frankfurt, Max-von-Laue-Strasse 1, 60438 Frankfurt am Main, Germany*

(Received 30 October 2015; revised manuscript received 20 April 2016; published 7 June 2016)

We report on a combined theoretical and experimental investigation of the superconducting state in the quasi-two-dimensional organic superconductor κ-$(ET)_2Cu[N(CN)_2]Br$. Applying spin-fluctuation theory to a low-energy, material-specific Hamiltonian derived from *ab initio* density functional theory we calculate the quasiparticle density of states in the superconducting state. We find a distinct three-peak structure that results from a strongly anisotropic mixed-symmetry superconducting gap with eight nodes and twofold rotational symmetry. This theoretical prediction is supported by low-temperature scanning tunneling spectroscopy on *in situ* cleaved single crystals of κ-$(ET)_2Cu[N(CN)_2]Br$ with the tunneling direction parallel to the layered structure.

DOI: 10.1103/PhysRevLett.116.237001

Introduction.—It has been widely accepted that κ-$(ET)_2X$ organic charge-transfer salts [where ET denotes bis(ethylenedithio)tetrathiafulvalene and X a monovalent anion] share essential features with cuprates regarding their superconducting state [1]. In both classes of materials, the electronic structure is quasi two dimensional and superconductivity emerges in the vicinity of an antiferromagnetically ordered Mott insulating phase. The transformation of these Mott insulators into superconductors can be achieved either by doping (cuprates) or by increasing the bandwidth (organics) through the application of physical or chemically induced pressure, see, e.g., Ref. [2]. In view of these similarities, it is natural to investigate whether a related coupling mechanism is operative in both classes of materials.

A direct determination of the pairing mechanism is extremely difficult, if not impossible, and therefore most efforts have been directed towards the determination of the symmetry of the superconducting energy gap function. For the cuprates, thanks to the availability of phase-sensitive probes, compelling evidence was provided early on that the gap has predominantly $d_{x^2-y^2}$ symmetry [3,4]. The lack of such probes for the organic charge-transfer salts, rooted in difficulties in proper material preparation, makes the situation less clear. There has been a long-lasting controversy about the gap symmetry in the most widely studied materials κ-$(ET)_2Cu[N(CN)_2]Br$ (for short, κ-Br) and κ-$(ET)_2Cu(NCS)_2$ (κ-NCS), with some results in support of an *s*-wave and others consistent with a *d*-wave scenario (see the reviews [2,5–7] for the status of the discussion up until 2006). More recent attempts include magnetocalorimetry [8], surface impedance [9], and high-resolution specific heat measurements [10,11], both in favor of *d*-wave pairing, even though earlier results of the specific heat favored *s*-wave symmetry [12–14]. On the other hand, by analyzing measurements of elastic constants [15] a mixed order parameter of either $A_{1g} + B_{1g}$ or $B_{2g} + B_{3g}$ has been claimed for κ-Br following the classification of irreducible representations of the material's orthorhombic D_{2h} point group.

In the above-mentioned studies, the gap function could be determined only indirectly from the temperature dependence of the quantity investigated. By contrast, a direct examination of the energy gap and its angular dependence is possible, in principle, through scanning tunneling spectroscopy (STS). Such STS studies have been performed by tunneling either into *as grown* surfaces for κ-NCS [16] and κ-Br [17], or into *focused-ion-beam-cut* surfaces for partially deuterated κ-Br [18]. The results were found to be consistent with a *d*-wave order parameter. However, with the exception of Ref. [18], no surface characterization was provided in these studies.

In this Letter we report evidence for an anisotropic superconducting gap structure for κ-Br based on a combined theoretical and STS investigation. By first constructing a two-dimensional Hubbard model of the ET layer from *ab initio* density functional theory (DFT) calculations and subsequently applying spin-fluctuation theory to this model, we predict the presence of a strongly anisotropic superconducting gap. As a consequence of the orthorhombicity of the crystal structure and the resulting details of the electronic structure, the order parameter does not have pure *d*-wave symmetry. Instead, an eight-node twofold rotationally symmetric state is realized, which we identify as

(extended) $s + d_{x^2-y^2}$. This pairing symmetry results in a quasiparticle density of states (DOS) with a distinct three-peak structure. STS measurements performed on well-defined surfaces obtained from a recently developed *in situ* cleaving technique [19] support this theoretical finding.

Theory.—We performed *ab initio* DFT calculations for κ-Br on an all-electron full-potential local orbital [20] basis and subsequently derived a tight-binding model from projective molecular orbital Wannier functions [21,22]. The resulting low-energy Hamiltonian $H_0 = \sum_{ij} t_{ij}(c_i^\dagger c_j +$ H.c.), with hopping parameters t_{ij} between ET molecules at sites i and j, consists of four bands arising from the highest occupied molecular orbitals of the ET molecules in the crystallographic unit cell and is 3/4 filled (see Ref. [22]).

Previous theoretical approaches [23] approximated the real crystal structure by an anisotropic triangular lattice of $(ET)_2$ dimers [24]. This approximation was shown to be justified in the insulating phase of κ-$(ET)_2X$ materials [25], but not in the superconducting state [26]. Hence, our method, which is based on an *ab initio* derived Hamiltonian with the full symmetry of the ET layer, is more realistic than previous approaches.

In the following, we take the rigorous viewpoint that superconductivity in κ-Br is solely driven by electron-electron interactions, see, e.g., Refs. [2,27,28]. Therefore, we add an intramolecular Hubbard interaction term $H_{\rm int} = U\sum_i n_{i\uparrow} n_{i\downarrow}$ to H_0. In this setup, we calculate the optimal geometry of the superconducting gap function using random phase approximation (RPA) spin-fluctuation theory in the spin-singlet channel [29]. For computational details, see the Supplemental Material [30]. We stress, however, that our results do not exclude a contribution from electron-phonon interactions, indications of which have been found, e.g., in studies of the isotope effect [41] and phonon renormalization [42].

From the RPA calculation, we find that the superconducting order parameter has eight nodes [see Fig. 1(a)], in contrast to previous reports of pure d-wave states with four nodes [6,23]. The first set of nodes labeled α in Fig. 1(a) appears on the quasi-one-dimensional part of the Fermi surface. The four nodes on the elliptic part of the Fermi surface, denoted β in Fig. 1(a), are close to the Brillouin zone diagonals. The full angular dependence of the gap function is shown in Fig. 1(b). The angles corresponding to the node positions are $\varphi_\alpha \sim 15°$ and $\varphi_\beta \sim 58°$, all measured with respect to the k_x direction. Nodes at other angles are symmetry equivalent to α and β. The three maxima of the superconducting gap magnitude are indicated by A, B, and C in Fig. 1. The corresponding angles are $\varphi_A = 90°$, $\varphi_B = 45°$, and $\varphi_C = 0°$. Maxima at other angles are symmetry equivalent to A, B, and C.

The quasiparticle DOS $\rho_{\rm qp}(E)$ in the superconducting state can be calculated from the momentum structure of the superconducting gap $\Delta(\vec{k})$, as given in Eq. (1). A small

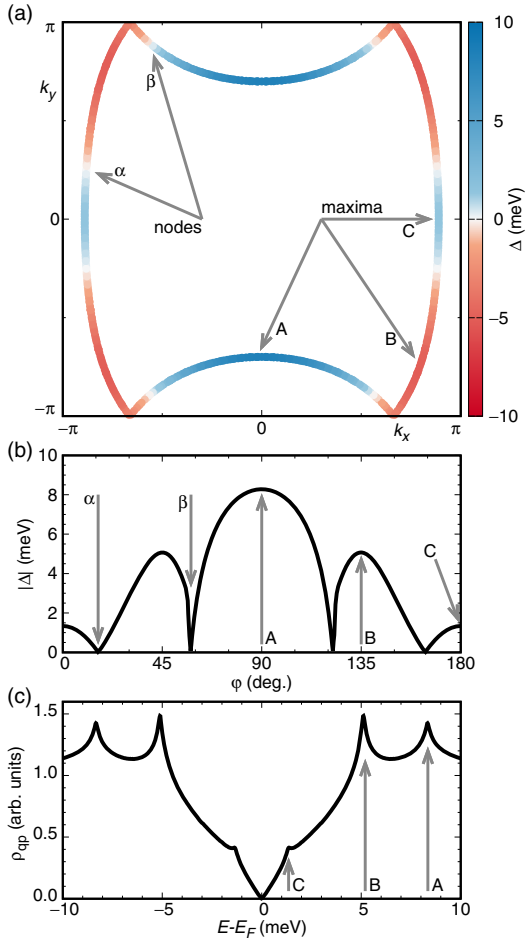

FIG. 1. *Ab initio* calculated results for (a) superconducting gap Δ on the Fermi surface, (b) absolute value $|\Delta|$ of the superconducting gap as a function of the angle φ in the $k_x k_y$ plane measured with respect to the k_x direction, and (c) quasiparticle DOS $\rho_{\rm qp}$ in the superconducting state of κ-Br. The maxima of the superconducting gap magnitude are indicated by arrows A, B, and C, while the positions of nodes are indicated by arrows α and β. The energy scale is set to $\Delta_0 = 10$ meV. A small broadening of $\Gamma = 0.07$ meV is included here.

broadening of the energy spectrum due to finite quasiparticle lifetimes is modeled by the parameter Γ [43]:

$$\rho_{\rm qp}(E,\Gamma) \propto \sum_{\vec{k}} {\rm Re}\frac{|E+i\Gamma|}{\sqrt{(E+i\Gamma)^2 - \Delta(\vec{k})^2}}. \qquad (1)$$

The main difference between our formulation [Eq. (1)] and conventional approaches [16–18] is that we do *not* assume the Fermi surface to be a concentric circle. Instead, we transform the usual angular integration (see Refs. [16–18] and the Supplemental Material [30]) into a sum over the discretized *ab initio* Fermi surface. Our approach can therefore discriminate between different d-wave solutions already on the level of the quasiparticle DOS. The approximations made in the derivation of Eq. (1) are

detailed in the Supplemental Material [30]. The quasiparticle DOS calculated from Eq. (1), using the gap calculated from a RPA for $\Delta(\vec{k})$, shows three distinct features [Fig. 1(c)] that correspond to the previously discussed gap maxima A, B, and C.

Experiment.—Single crystals of κ-Br were grown in an electrochemical crystallization process [44]. All investigations were performed with a commercial low-temperature scanning tunneling microscope (STM) under ultrahigh vacuum (UHV) conditions with a base pressure of about 5×10^{-11} mbar. In order to obtain a clean surface, as is essential for high-resolution STM investigations, we cleaved the crystal surface with a homebuilt cutter in UHV. After *in situ* cleaving, the sample was mounted into the precooled STM stage. Measurements have been performed on three single crystals, yielding essentially identical results.

By this procedure, the cooling rate of the sample, relevant at the glasslike ethylene–end group ordering transition T_g, is estimated to be about -1 K/min at $T_g \approx$ 75–80 K (see Ref. [45]). This implies a residual disorder in the orientational degrees of freedom of the ET molecules' terminal ethylene groups on the order of 3% [46,47]. For details on the STM and STS measurements, see Ref. [19].

Figure 2(a) shows a (30×30) nm^2 STM image of a κ-Br crystal cleaved perpendicularly to the molecular layers (for the parallel topography, see Refs. [19,48]). The STM image reveals a stripe pattern with an average width of 29.9 Å [see Fig. 2(b)], which is in good agreement with the lattice constant of κ-Br in the c direction. One period of the stripe pattern consists of two ET and two anion layers. For a better illustration, Fig. 2(b) shows the height profile along the white shaded area in Fig. 2(a), wherein the position of the anion layers is marked by red stripes. The height profile is mainly a mapping of the topographical surface profile, but it is also influenced by the local density of states. By analyzing the height profile along a single unit cell we conclude that the cutting plane is rotated by $\varphi_{ab} = 60°$ about the c axis with respect to the b axis (see Ref. [30]).

Next, we measured the differential conductance dI/dV of the ET layer and the anion layer in the temperature range from 5 to 13 K [see Figs. 2(c) and 2(d) for the data at 5 K] in order to extract information about their DOS. The dI/dV spectra have been normalized to the tunneling transmission function $T(V)$, which is almost linear in the measured energy range and accounts for a small asymmetry observed in the original spectra [49]. Assuming a constant DOS for the tip material, $(dI/dV)/T(V)$ is proportional to the differential conductance $D(V)$ of the sample.

The differential conductance is nonzero at $E = E_F$ for the spectrum measured parallel to the ET layer [Fig. 2(c)]. In contrast, the differential conductance spectrum measured at the anion layer [Fig. 2(d)] approaches zero at the Fermi edge $[dI/dV(E = E_F) \approx 0]$ indicating the expected insulating behavior. The V-shaped feature for $|eV| > 15$ meV results from a logarithmic suppression of the density of states at the

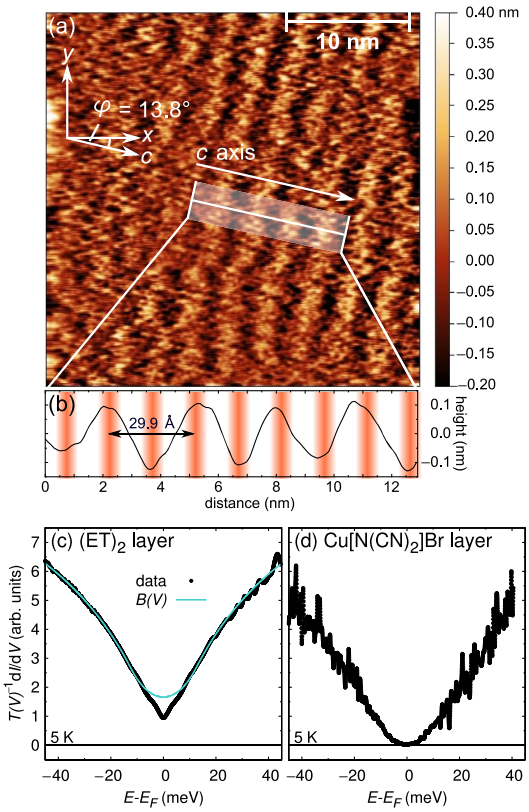

FIG. 2. (a) (30×30) nm^2 STM image of the crystal surface with a tunneling direction parallel to the layered structure of the κ-Br crystal, revealing a stripe pattern ($T = 5$ K, $I = 60$ pA, $U_{\text{tip}} = 30$ mV). (b) The height profile along the marked area in (a) reveals an average stripe width of 29.9 Å. The red stripes indicate the position of the insulating layers. (c) Conductance spectra $dI/dV/T(V)$ at $T = 5$ K (the black dots) measured at the ET layer and (d) the Cu$[\text{N(CN)}_2]$Br layer with $-eU_{\text{tip}} = eV = E - E_F$. The function $B(V)$ is also plotted in (c) (see the text for a discussion).

Fermi edge described by a function $B(V)$ [see Fig. 2(c)], which has been assigned to electronic disorder [19]. Temperature-dependent measurements up to 13 K (see the Supplemental Material [30]) show a nearly temperature-independent function for the DOS $B(V)$ as described in Refs. [19,50].

An important piece of information is obtained from the second derivative of dI/dV with respect to the voltage, as presented in Fig. 3(a). This function at $T = 5$ K shows three pairs of narrow minima (denoted as A, B, and C), which correspond to superconducting coherence peaks and will be discussed further below. The pronounced maximum at E_F reflects the zero-bias anomaly of the normal-state DOS [19].

The conductance spectrum related to the superconducting phase is given by $S(V) = [B(V)T(V)]^{-1}dI/dV$. In Fig. 3(b), $S(V)$ measured parallel to the layered crystal structure is plotted for temperatures between 5 and 13 K. The two main features in the second derivative [shown by arrows A and B in Fig. 3(b)] are already visible in the bare

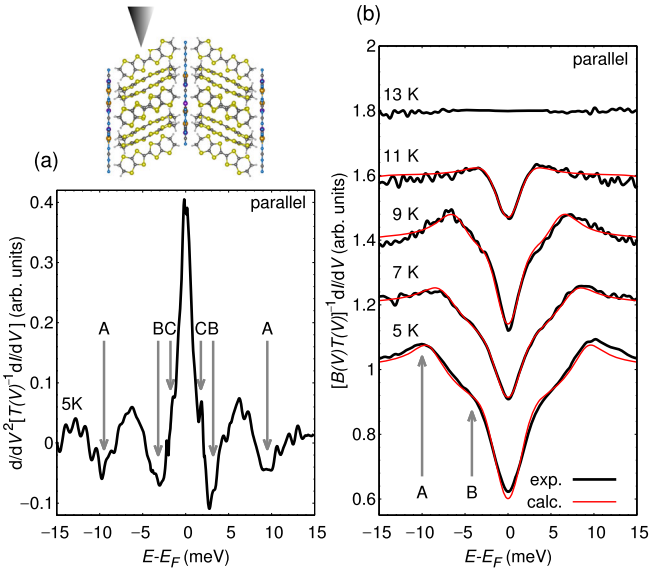

FIG. 3. (a) Second derivative of the conductance spectrum $dI/dV/T(V)$ at $T = 5$ K shown in Fig. 2(c). Arrows labeled by A, B, and C indicate three pairs of minima which are symmetric to the origin, corresponding to the coherence peaks partially seen in (b). (b) Conductance spectra $S(V) = 1/[B(V)T(V)]dI/dV$ of the superconducting state as a function of $eV = E - E_F$ at different temperatures measured parallel to the layered crystal structure. The red lines show mappings of Eq. (2) to the measured data.

conductance spectra, whereas feature C becomes discernible only in the second derivative of the spectra.

Discussion.—Our theoretical calculations predict an anisotropic superconducting order parameter. We note that a very accurate representation of the calculated gap on the Fermi surface is given in terms of extended s- and d-wave functions (see also the Supplemental Material [30]): $\Delta(\vec{k}) = \Delta_0[c_{s_1}(\cos k_x + \cos k_y) + c_{d_1}(\cos k_x - \cos k_y) + c_{s_2}(\cos k_x \cos k_y)]$. Although our experiments resolve the existence of feature C only in the second derivative of the conductance, the shape of the experimental tunneling spectra [Fig. 3(b)] bears the essential features predicted by our theory [Fig. 1(c)]. Features A and B are only slightly shifted with respect to each other.

In order to connect the calculated quasiparticle DOS [Eq. (1)] to the measured spectrum $S(V)$, we investigate whether quantitative agreement can be reached by fine-tuning some parameters. In this process, the symmetry of the superconducting state is kept fixed to the theoretical prediction (mixed extended $s + d_{x^2-y^2}$). We calculate $S(V)$ from Eq. (2) (see the Supplemental Material [30]), where $f(E)$ is the Fermi function, V is the bias voltage, and x is a background shift, which accounts for parasitic conduction paths:

$$S(V) = \frac{1}{B(V)T(V)}\frac{dI(V)}{dV} \propto \int_{-\infty}^{\infty} dE[\rho_{\mathrm{qp}}(E)(1-x)+x]\frac{-df(E+eV)}{dV}. \quad (2)$$

TABLE I. Values of the parameters in Eq. (2) obtained by mapping the calculated $S(V)$ to the experimental spectra.

T (K)	c_{s_1}	c_{d_1}	c_{s_2}	Δ_0 (meV)	Γ (meV)	x
5	−0.109	−0.276	−0.615	12.218	0.690	0.520
7	−0.128	−0.280	−0.592	10.638	0.641	0.603
9	−0.064	−0.317	−0.620	7.376	0.000	0.466
11	−0.158	−0.200	−0.642	2.984	0.035	0.188

Using the expression for $\Delta(\vec{k})$ given above, we reevaluate Eqs. (1) and (2) with parameter sets $\{\Delta_0, c_{s_1}, c_{d_1}, c_{s_2}, x, \Gamma\}$ until optimal agreement with the experimental spectra in the interval $[-12, +12]$ meV is reached. The corresponding calculated spectra are shown in Fig. 3(b) as solid red lines. The optimal parameter values listed in Table I are consistent throughout the investigated parameter range. Only the origin of the nonmonotonic behavior of Γ is currently unclear.

The nodal positions we find in our study are particularly appealing because of the ongoing controversy about the realization of either d_{xy} or $d_{x^2-y^2}$ pairing in quasi-2D organic superconductors. In previous works, a fourfold rotational symmetry constraint was introduced based on single-band Hubbard-type models proposed for these systems with a dimer of molecules per site on an anisotropic triangular lattice [23,25,51–53]. Inspired by recent *ab initio* studies [54,55], we, however, went back to the original κ-type lattice structure and treated all molecules as entities. As a consequence, we find evidence for a mixed-symmetry extended $s + d_{x^2-y^2}$ state, which has been suggested to exist in some parameter regions of various models for κ-type charge-transfer salts [26,56,57], but which has so far not been shown to exist in a material-specific Hamiltonian. Interestingly, a different kind of eight-node superconductivity has been recently proposed in the context of Fe-based superconductors [58].

The nodes β correspond to the usually discussed $d_{x^2-y^2}$ solution, while the nodes α lie close to the k_x direction. In contrast to the d_{xy} gap found in Ref. [23] there are no nodes along the k_y direction in our results. The twofold rotational symmetry found in our study is very important because the analysis of many experiments on κ-$(\mathrm{ET})_2X$ materials is based, possibly mistakenly, on the subtraction of a large twofold symmetric alleged background (see Refs. [8,59]) attributed to other effects, such as phonons.

We note that from a study of the suppression of T_c with increasing disorder in κ-NCS, a mixed order parameter has been suggested as an important constraint on models of the superconductivity [60]. The anisotropic gap should also appear in related physical properties, such as the electronic part of the specific heat. Calculations of the electronic contribution to the specific heat based on the gap function determined in this work are in favorable agreement with experimental observations; see the Supplemental Material [30].

Summary.—We have studied the organic superconductor κ-$(ET)_2Cu[N(CN)_2]Br$ in RPA spin-fluctuation theory based on *ab initio* density functional theory calculations, as well as low-temperature scanning tunneling microscopy and spectroscopy with the tunneling direction parallel to the layered structure. In both theory and experiment, we find evidence for three coherence peaks in the spectra of the superconducting state. Our results indicate that the symmetry of the superconducting pairing in κ-$(ET)_2X$ organics might be neither of the d_{xy} and $d_{x^2-y^2}$ states discussed in previous studies, but rather a mixed extended $s + d_{x^2-y^2}$ type with four nodes located close to the Brillouin zone diagonals and four nodes located on the quasi-1D sheets.

We thank the German Research Foundation (Deutsche Forschungsgemeinschaft, SFB/TR 49) and the Graduate School Materials Science in Mainz for their financial support. D. G. acknowledges the helpful discussions with Andreas Kreisel, Peter J. Hirschfeld, and Paul C. Canfield. Calculations were performed on the LOEWE-CSC and FUCHS supercomputers of the Center for Scientific Computing (CSC) in Frankfurt am Main, Germany.

*elmers@uni-mainz.de

[1] R. H. McKenzie, Similarities between organic and cuprate superconductors, Science **278**, 820 (1997).

[2] N. Toyota, M. Lang, and J. Müller, *Low-Dimensional Molecular Metals* (Springer-Verlag, Berlin, 2007).

[3] D. J. Van Harlingen, Phase-sensitive tests of the symmetry of the pairing state in the high-temperature superconductors —Evidence for $d_{x^2-y^2}$ symmetry, Rev. Mod. Phys. **67**, 515 (1995).

[4] C. C. Tsuei and J. R. Kirtley, Pairing symmetry in cuprate superconductors, Rev. Mod. Phys. **72**, 969 (2000).

[5] M. Lang and J. Müller, in *The Physics of Superconductors*, Vol. II, edited by K. H. Bennemann and J. B. Ketterson (Springer-Verlag, Berlin, 2004).

[6] K. Kuroki, Pairing symmetry competition in organic superconductors, J. Phys. Soc. Jpn. **75**, 051013 (2006).

[7] B. Powell and R. H. McKenzie, Strong electronic correlations in superconducting organic charge transfer salts, J. Phys. Condens. Matter **18**, R827 (2006).

[8] L. Malone, O. J. Taylor, J. A. Schlueter, and A. Carrington, Location of gap nodes in the organic superconductors κ-$(ET)_2Cu(NCS)_2$ and κ-$(ET)_2Cu[N(CN)_2]Br$ determined by magnetocalorimetry, Phys. Rev. B **82**, 014522 (2010).

[9] S. Milbradt, A. A. Bardin, C. J. S. Truncik, W. A. Huttema, A. C. Jacko, P. L. Burn, S. C. Lo, B. J. Powell, and D. M. Broun, In-plane superfluid density and microwave conductivity of the organic superconductor κ-$(ET)_2Cu[N(CN)_2]Br$: Evidence for *d*-wave pairing and resilient quasiparticles, Phys. Rev. B **88**, 064501 (2013).

[10] O. J. Taylor, A. Carrington, and J. A. Schlueter, Specific-Heat Measurements of the Gap Structure of the Organic Superconductors κ-$(ET)_2Cu[N(CN)_2]Br$ and κ-$(ET)_2Cu(NCS)_2$, Phys. Rev. Lett. **99**, 057001 (2007).

[11] O. J. Taylor, A. Carrington, and J. A. Schlueter, Superconductor-insulator phase separation induced by rapid cooling of κ-$(ET)_2Cu[N(CN)_2]Br$, Phys. Rev. B **77**, 060503(R) (2008).

[12] H. Elsinger, J. Wosnitza, S. Wanka, J. Hagel, D. Schweitzer, and W. Strunz, κ-$(BEDT\text{-}TTF)_2Cu[N(CN)_2]Br$: A Fully Gapped Strong-Coupling Superconductor, Phys. Rev. Lett. **84**, 6098 (2000).

[13] J. Müller, M. Lang, R. Helfrich, R. Steglich, and T. Sasaki, High-resolution ac-calorimetry studies of the quasi-two-dimensional organic superconductor κ-$(BEDT\text{-}TTF)_2Cu(NCS)_2$, Phys. Rev. B **65**, 140509(R) (2002).

[14] J. Wosnitza, S. Wanka, J. Hagel, M. Reibelt, D. Schweitzer, and J. A. Schlueter, Thermodynamic properties of quasi-two-dimensional organic superconductors, Synth. Met. **133–134**, 201 (2003).

[15] M. Dion, D. Fournier, M. Poirier, K. D. Truong, and A.-M. S. Tremblay, Mixed pairing symmetry in κ-$(BEDT\text{-}TTF)_2X$ organic superconductors from ultrasonic velocity measurements, Phys. Rev. B **80**, 220511(R) (2009).

[16] T. Arai, K. Ichimura, K. Nomura, S. Takasaki, J. Yamada, S. Nakatsuji, and H. Anzai, Tunneling spectroscopy on the organic superconductor κ-$(BEDT\text{-}TTF)_2Cu(NCS)_2$ using STM, Phys. Rev. B **63**, 104518 (2001).

[17] K. Ichimura, M. Takami, and K. Nomura, Direct observation of *d*-wave superconducting gap in κ-$(ET)_2Cu[N(CN)_2]Br$ with scanning tunneling microscopy, J. Phys. Soc. Jpn. **77**, 114707 (2008).

[18] Y. Oka, H. Nobukane, N. Matsunaga, K. Nomura, K. Katono, K. Ichimura, and A. Kawamoto, Tunneling spectroscopy in organic superconductor κ-$(BEDT\text{-}TTF\text{-}d[3,3])_2Cu[N(CN)_2]Br$, J. Phys. Soc. Jpn. **84**, 064713 (2015).

[19] S. Diehl, T. Methfessel, U. Tutsch, J. Müller, M. Lang, M. Huth, M. Jourdan, and H. J. Elmers, Disorder-induced gap in the normal density of states of the organic superconductor κ-$(BEDT\text{-}TTF)_2Cu[N(CN)_2]Br$, J. Phys. Condens. Matter **27**, 265601 (2015).

[20] K. Koepernik and H. Eschrig, Full-potential nonorthogonal local-orbital minimum-basis band-structure scheme, Phys. Rev. B **59**, 1743 (1999); see also http://www.FPLO.de.

[21] H. Eschrig and K. Koepernik, Tight-binding models for the iron-based superconductors, Phys. Rev. B **80**, 104503 (2009).

[22] D. Guterding, R. Valentí, and H. O. Jeschke, Influence of molecular conformations on the electronic structure of organic charge transfer salts, Phys. Rev. B **92**, 081109(R) (2015); in this Letter we use the model for κ-Br in ground state conformation (eclipsed) of the ET molecules and relabel the crystal axes (*a*, *b*, *c*) as (*b*, *c*, *a*).

[23] J. Schmalian, Pairing due to Spin Fluctuations in Layered Organic Superconductors, Phys. Rev. Lett. **81**, 4232 (1998).

[24] For the difference in hopping structure, see, for instance, Fig. 1(a) and Fig. 13 in Ref. [25] or Fig. 1 in Ref. [53].

[25] H. Kino and H. Fukuyama, Phase diagram of two-dimensional organic conductors: $(BEDT\text{-}TTF)_2X$, J. Phys. Soc. Jpn. **65**, 2158 (1996).

[26] K. Kuroki, T. Kimura, R. Arita, Y. Tanaka, and Y. Matsuda, $d_{x^2-y^2}$- versus d_{xy}-like pairings in organic superconductors κ-$(BEDT\text{-}TTF)_2X$, Phys. Rev. B **65**, 100516(R) (2002).

[27] A. Ardavan, S. Brown, S. Kagoshima, K. Kanoda, K. Kuroki, H. Mori, M. Ogata, S. Uji, and J. Wosnitza, Recent topics of organic superconductors, J. Phys. Soc. Jpn. **81**, 011004 (2012).

[28] E. Yusuf, B. J. Powell, and R. H. McKenzie, Antiferromagnetic spin fluctuations in the metallic phase of quasi-two-dimensional organic superconductors, Phys. Rev. B **75**, 214515 (2007).

[29] S. Graser, T. A. Maier, P. J. Hirschfeld, and D. J. Scalapino, Near-degeneracy of several pairing channels in multiorbital models for the Fe pnictides, New J. Phys. **11**, 025016 (2009).

[30] See Supplemental Material at http://link.aps.org/supplemental/10.1103/PhysRevLett.116.237001, which includes Refs. [31–40], for details on experimental crystal orientation, experimental extraction of the superconducting density of states, and an analysis of high-resolution specific heat data. We explain the computational formalism, including the RPA spin-fluctuation calculations, and present a robustness analysis for the fitting procedures.

[31] K. Fujita, I. Grigorenko, J. Lee, J. X. Zhu, J. C. Davis, H. Eisaki, S. Uchida, and A. V. Balatsky, Bogoliubov angle and visualization of particle-hole mixtures in superconductors, Phys. Rev. B **78**, 054510 (2008).

[32] P. E. Blöchl, O. Jepsen, and O. K. Andersen, Improved tetrahedron method for Brillouin-zone integrations, Phys. Rev. B **49**, 16223 (1994).

[33] U. Geiser, A. J. Schultz, H. W. Wang, D. M. Watkins, D. L. Stupka, J. M. Williams, J. E. Schirber, D. L. Overmeyer, D. Jung, J. J. Novoa, and M.-H. Whangbo, Strain index, lattice softness and superconductivity of organic donor-molecule salts: Crystal and electronic structures of three isostructural salts κ-$(BEDT\text{-}TTF)_2Cu[N(CN)_2]X$ (X = Cl, Br, I), Physica (Amsterdam) **174C**, 475 (1990).

[34] J. P. Perdew, K. Burke, and M. Ernzerhof, Generalized Gradient Approximation Made Simple, Phys. Rev. Lett. **77**, 3865 (1996).

[35] D. Guterding, H. O. Jeschke, P. J. Hirschfeld, and R. Valentí, Unified picture of the doping dependence of superconducting transition temperatures in alkali metal/ammonia intercalated FeSe, Phys. Rev. B **91**, 041112(R) (2015).

[36] D. Guterding, S. Backes, H. O. Jeschke, and R. Valentí, Origin of the superconducting state in the collapsed tetragonal phase of KFe_2As_2, Phys. Rev. B **91**, 140503 (R) (2015).

[37] N. E. Bickers, D. J. Scalapino, and S. R. White, Conserving Approximations for Strongly Correlated Electron Systems: Bethe-Salpeter Equation and Dynamics for the Two-Dimensional Hubbard Model, Phys. Rev. Lett. **62**, 961 (1989).

[38] D. J. Scalapino, E. Loh, Jr., and J. E. Hirsch, *d*-wave pairing near a spin-density-wave instability, Phys. Rev. B **34**, 8190 (1986).

[39] A. Savitzky and M. J. E. Golay, Smoothing and differentiation of data by simplified least squares procedures, Anal. Chem. **36**, 1627 (1964).

[40] H. Padamsee, J. E. Neighbor, and C. A. Shiffman, Quasiparticle phenomenology for thermodynamics of strong-coupling superconductors, J. Low Temp. Phys. **12**, 387 (1973).

[41] A. M. Kini, K. D. Carlson, J. D. Dudek, U. Geiser, H. H. Wang, and J. M. Williams, Isotope effect in BEDT-TTF based organic superconductors, Synth. Met. **85**, 1617 (1997).

[42] L. Pintschovius, H. Rietschel, T. Sasaki, H. Mori, S. Tanaka, N. Toyota, M. Lang, and F. Steglich, Observation of superconductivity-induced phonon frequency changes in the organic superconductor κ-$(BEDT\text{-}TTF)_2Cu(NCS)_2$, Europhys. Lett. **37**, 627 (1997).

[43] R. C. Dynes, V. Narayanamurti, and J. P. Garno, Direct Measurement of Quasiparticle-Lifetime Broadening in a Strong-Coupled Superconductor, Phys. Rev. Lett. **41**, 1509 (1978).

[44] H. Anzai, J. M. Delrieu, S. Takasaki, S. Nakatsuji, and J. Yamada, Crystal growth of organic charge-transfer complexes by electrocrystallization with controlled applied current, J. Cryst. Growth **154**, 145 (1995).

[45] J. Müller, M. Lang, F. Steglich, J. A. Schlueter, A. M. Kini, and T. Sasaki, Evidence for structural and electronic instabilities at intermediate temperatures in κ-$(BEDT\text{-}TTF)_2X$ for $X = Cu[N(CN)_2]Cl$, $Cu[N(CN)_2Br$ and $Cu(NCS)_2$: Implications for the phase diagram of these quasi-two-dimensional organic superconductors, Phys. Rev. B **65**, 144521 (2002).

[46] B. Hartmann, J. Müller, and T. Sasaki, Mott metal-insulator transition induced by utilizing a glasslike structural ordering in low-dimensional molecular conductors, Phys. Rev. B **90**, 195150 (2014).

[47] J. Müller, B. Hartmann, R. Rommel, J. Brandenburg, S. M. Winter, and J. A. Schlueter, Origin of the glasslike dynamics in molecular metals κ-$(BEDTTTF)_2X$: Implications from fluctuation spectroscopy and *ab initio* calculations, New J. Phys. **17**, 083057 (2015).

[48] T. Burgin, T. Miebach, J. C. Huffman, L. K. Montgomery, J. A. Paradis, C. Rovira, M.-H. Whangbo, S. N. Magonov, S. I. Khan, C. E. Strouse, D. L. Overmyer, and J. E. Schirber, 20 K crystal structure, electrical transport, electronic band structure, scanning tunnelling microscopy and pressure-RF impedance studies on the organic conducting salt κ-$(BEDT\text{-}TSF)_2Cu[N(CN)_2]Br$, J. Mater. Chem. **5**, 1659 (1995).

[49] V. A. Ukraintsev, Data evaluation technique for electron-tunneling spectroscopy, Phys. Rev. B **53**, 11176 (1996).

[50] H. Shinaoka and M. Imada, Single-particle excitations under coexisting electron correlation and disorder: A numerical study of the Anderson-Hubbard model, J. Phys. Soc. Jpn. **78**, 094708 (2009).

[51] R. H. McKenzie, A strongly correlated electron model for the layered organic superconductors κ-$(BEDT\text{-}TTF)_2X$, Comments Condens. Matter Phys. **18**, 309 (1998).

[52] M. Zehetmayer, A review of two-band superconductivity: Materials and effects on the thermodynamic and reversible mixed-state properties, Supercond. Sci. Technol. **26**, 043001 (2013).

[53] H. C. Kandpal, I. Opahle, Y.-Z. Zhang, H. O. Jeschke, and R. Valentí, Revision of Model Parameters for κ-Type Charge Transfer Salts: An *Ab Initio* Study, Phys. Rev. Lett. **103**, 067004 (2009).

[54] K. Nakamura, Y. Yoshimoto, and M. Imada, *Ab initio* two-dimensional multiband low-energy models of

$EtMe_3Sb[Pd(dmit)_2]_2$ and κ-$(BEDT\text{-}TTF)_2Cu(NCS)_2$ with comparisons to single-band models, Phys. Rev. B **86**, 205117 (2012).

[55] M. Altmeyer, R. Valentí, and H. O. Jeschke, Role of layer packing for the electronic properties of the organic superconductor $(BEDT\text{-}TTF)_2Ag(CF_3)_4(TCE)$, Phys. Rev. B **91**, 245137 (2015).

[56] B. J. Powell and R. H. McKenzie, Symmetry of the Superconducting Order Parameter in Frustrated Systems Determined by the Spatial Anisotropy of Spin Correlations, Phys. Rev. Lett. **98**, 027005 (2007).

[57] T. Watanabe, H. Yokoyama, Y. Tanaka, and J. Inoue, Predominant magnetic states in the Hubbard model on anisotropic triangular lattices, Phys. Rev. B **77**, 214505 (2008).

[58] K. Okazaki *et al.*, Octet-line node structure of superconducting order parameter in KFe_2As_2, Science **337**, 1314 (2012).

[59] K. Izawa, H. Yamaguchi, T. Sasaki, and Y. Matsuda, Superconducting Gap Structure of κ-$(BEDT\text{-}TTF)_2Cu(SCN)_2$ Probed by Thermal Conductivity Tensor, Phys. Rev. Lett. **88**, 027002 (2001).

[60] J. G. Analytis, A. Ardavan, S. J. Blundell, R. L. Owen, E. F. Garman, C. Jeynes, and B. J. Powell, Effect of Irradiation-Induced Disorder on the Conductivity and Critical Temperature of the Organic Superconductor κ-$(BEDT\text{-}TTF)_2Cu(SCN)_2$, Phys. Rev. Lett. **96**, 177002 (2006).